

Numerical Simulation of the Air Flow and Thermal Comfort in a Train Cabin

M. Konstantinov¹ and C. Wagner^{1,2}

¹Institute of Thermodynamics and Fluid Mechanics
University of Technology Ilmenau, Germany

²Institute of Aerodynamics and Flow Technology
German Aerospace Center, Göttingen, Germany

Abstract

Results of numerical simulations of the air flow including the heat transport and the thermal radiation as well as the thermal comfort of passengers in a train cabin are presented. The computations have been performed by coupling flow simulations conducted with the computational fluid dynamics (CFD) code OpenFOAM with finite-element simulations of the heat transport within the passengers using the code THESEUS-FE. With the latter the bodies of passengers were modelled based on various layers with different heat transport characteristics to account for effects like blood flow, heat transfer through the skin and the clothing as well as activity levels and ambient humidity. With these computations we simulated and analysed the thermal comfort of passengers in the cabin of DLRs concept train called next generation train (NGT).

Keywords: thermal comfort model (TCM), CFD, cabin air flow, Fiala-Manikin-Model.

1 Introduction

The thermal comfort and the well-being of passengers is an important criterion for train manufacturers. The thermal comfort of passengers in particular is influenced by the air flow, the temperature distribution and the thermal radiation in a specific cabin configuration. For the prediction of these processes numerous thermal sources have to be taking into account, one of which is the passenger itself. Conventionally, in computations using Computational Fluid Dynamics (CFD) methods, the thermal boundary conditions are prescribed at the passenger/cabin air interface in terms of either the specified heat flux or an isothermal temperature distribution. In this respect, the passenger is considered as a passive heat source [1-3]. There are also more sophisticated thermal comfort models, which consider the human body to consist of several layers with different heat conductivities and capacities and take into account the heat transport in the cardiovascular system and the influence of the

clothing. Additionally, the influence of the human activity level and of the ambient humidity on the human's physiology is considered, albeit in empirical form.

The thermal comfort simulations presented below are performed by coupling the finite volume method OpenFOAM, which solves the Reynolds-Averaged Navier-Stokes (RANS) equations using the Boussinesq approximation with the commercial finite element program, THESEUS-FE, developed by P+Z Engineering GmbH (FIALA-Manikin-Model) [4]. The model implemented in the latter considers all relevant thermo-physiological effects of a human body as described by D. Fiala et al. [5-6]. It calculates the so-called Zhang local sensation indices, which reflect the perceived temperature in a range from "very cold" to "very hot" [7]. Based on the latter, the Zhang local comfort index is evaluated, describing the perceived comfort in a range from "very uncomfortable" to "very comfortable" [8]. Using this coupled approach, computations of the flow and thermal comfort of passengers in the cabin of the Next Generation Train II (NGTII) have been performed and are discussed below. While the cabin of the NGTII-wagon consist of an upper and a lower level, only the results obtained for the upper part will be discussed in the following.

2 Thermal Comfort Model

The heat transport simulations conducted with the THESEUS-FE software [4] are based on a thermal manikin, the so-called FIALA-Manikin Model. The body of the latter consists of 54 body segments which we clustered to reduce their number to 14 segments. For example, we merged the head, face and neck of the FIALA-Manikin to one segment of our Thermal Comfort Model (TCM). Other clustered segments are the torso, and the left and right segments of the upper and lower arms, hands, upper and lower legs and feet. Each of these body segments consist of several material layers. Additionally, it is possible to define an individual clothing layer for any of the above discussed segments. Finally, it must be noted that the core of each segment has its own attributes and that gender effects as well as differences in the human thermoregulation are not considered.

For each body segment the following partial differential equation is solved in all layers to describe the temperature changes in each material element:

$$\rho c \frac{\partial T}{\partial t} = k \left(\frac{\partial^2 T}{\partial r^2} + \frac{\omega}{r} \frac{\partial T}{\partial r} \right) + q_m + \rho_b c_b w_b (T_{b,a} - T) \quad (1)$$

Here ρ is the density, c – the specific heat, k – the thermal conductivity, T – the temperature, q_m – the metabolic heat flow density, w_b – the blood perfusion rate and $T_{b,a}$ – the calculated arterial temperature. The term $\rho_b c_b w_b (T_{b,a} - T)$ describes the contribution due to the arterial blood flow. Blood circulation is of vital importance for the heat distribution within the human body [5-6]. The brain temperature, for example, would reach unrealistic values of more than 70°C in simulations which do not model the blood circulation. The shape of the body elements is simplified by considering them as cylinders with the exception of the head (sphere) where r is the radial coordinate of a body element. The dimensionless parameter ω is 1 for cylindrical body elements (for example the legs) and 2 for the spherical body

element (head). Thus, equation (1) describes the law of energy conservation for each finite element in the material layers representing the skin, fat, muscles, bones, brain and so on.

The local clothing properties of each garment are prescribed according to the model of McCullough [9]. The clothing is defined through the thickness, clothing resistance, evaporation resistance, non-structural mass and specific heat. The thickness of 3 mm has been chosen for torso, arms and legs, the thickness of 6 mm has been chosen for feet. For all dressed elements a clothing resistance 1.51 clo (1 clo = 0.155 m²K/W) was prescribed with the exception of feet (3.02 clo). We verified these clothing parameters in thermal comfort simulations performed for the cabins of the Airbus A320 and that of test facility Do728 [10]. From the computed surface (T_{sf}) and skin (T_{sk}) temperatures, the former is of major importance for the evaluation of the comfort indices. First, an equivalent temperature T_{eq} is determined according to

$$T_{eq} = T_{sf} - \frac{R + C + E}{h_{cal}}, \quad (2)$$

where R , C and E symbolize the heat fluxes caused by radiation, convection and evaporation. Evaporation is estimated and calculated in THESEUS-FE based on a prescribed humidity. Further, h_{cal} denotes the combined heat transfer coefficient of the specific environment ($h_r + h_c$), where h_r denotes the radiation and h_c the convection heat transfer coefficient. The equivalent temperature is the temperature of a homogeneous room with a radiation background temperature equal to the air temperature and low relative air speed.

The equivalent temperature and any other comfort index (e.g. both Zhang indices) were calculated by THESEUS, while the Zhang local sensation index (SI) is defined as a function of the following parameters

$$SI = f\left(T_{sk,i}, \frac{dT_{sk,i}}{dt}, \bar{T}_{sk,i}, \dot{T}_{hy}\right), \quad (3)$$

where $T_{sk,i}$ is the skin temperature of the body segment i and T_{hy} – the hypothalamus temperature. The resulting sensation scale ranges from: 4 – “very hot”, 3 – “hot”, 2 – “warm”, 1 – “slightly warm”, 0 – “neutral”, -1 – “slightly cool”, -2 – “cool”, -3 – “cold”, -4 – “very cold”.

Based on equation (3) the Zhang local thermal comfort index (Lc) is computed taking into account the overall thermal sensation (So)

$$Lc_i = f(SI_i, So) \quad (4)$$

The Zhang local comfort index ranges from 4 (“very comfortable”), 2 (“comfortable”), 0 (“just comfortable”) to -2 (“uncomfortable”), -4 (“very uncomfortable”). For more details on the calculation of the comfort indices and So specifically, the reader is referred to [8].

3 Thermal Comfort Calculation

To exchange data between the RANS simulations (with OpenFOAM) and the thermal comfort computation (with THESEUS-FE) we developed an interface. The interaction between OpenFOAM and THESEUS-FE realized with this interface is sketched in Fig. 1.

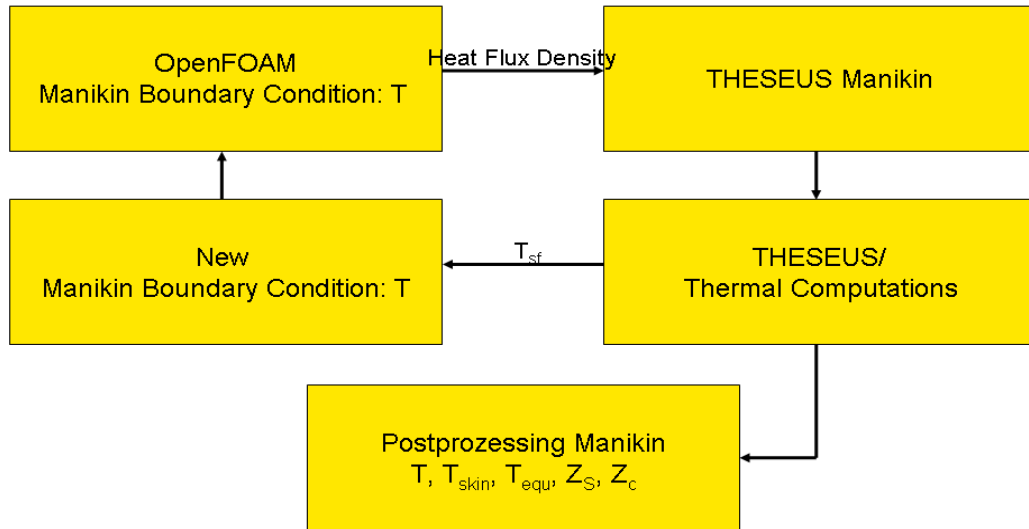


Figure 1: Implementation of the interface between OpenFOAM and THESEUS-FE

At the beginning of the simulations, the initial temperature on the surfaces of all body segments of the passengers is prescribed as follows: head – $T_{he} = 308$ K, torso – $T_t = 308$ K, upper arms – $T_{ua} = 306$ K, lower arms – $T_{la} = 306$ K, hands – $T_{ha} = 307$ K, upper legs – $T_{ul} = 305$ K, lower legs – $T_{ll} = 304$ K and feet – $T_{fo} = 304$ K. After 100 iterations the heat flux densities resulting from heat radiation and convection are computed and written to an output file. Reading this file, THESEUS-FE obtains the heat flux densities and calculates a new set of surface temperature boundary conditions by solving Eq. (1). The results can be interpreted as an estimate of the response of a typical human body to the specified thermal loading. Further, an “equivalent” temperature is computed which is used to assess the thermal comfort, as well as the surface (and skin) temperatures. The latter are then passed on to the RANS simulations by updating the surface temperature boundary condition through an intermediate output file. The whole procedure is repeated every 10 iterations of the RANS computations. The major part of the exchanged heat of the human is the dry heat flux which is calculated and handed over to THESEUS-FE. Additionally the humidity is set manually in the THESEUS input file.

4 Numerical Results

Solving the RANS equations with the finite volume method OpenFOAM the air flow in the train cabin has been investigated. Before, for the complete volume of the upper level of the Next Generation Train II wagon with 16 rows and 48 passengers a hybrid structured/unstructured mesh consisting of a total of 25 million cells has been generated using the mesher of the commercial program StarCCM+. The upper cabin of the Next Generation Train II and the mesh cross-sections are presented in Fig. 2.

For all passengers in the train cabin, i.e. $14 \times 48 = 672$, separate body segment boundary conditions were specified. Additionally, at both air inlet planes the volume flux of $0.33 \text{ m}^3/\text{s}$ and the temperature of 20 C° was prescribed. The walls representing the sides, bottom, ceiling and windows were assumed to be adiabatic. For the light-band the heat flux density of $100 \text{ W}/\text{m}^2$ was prescribed.

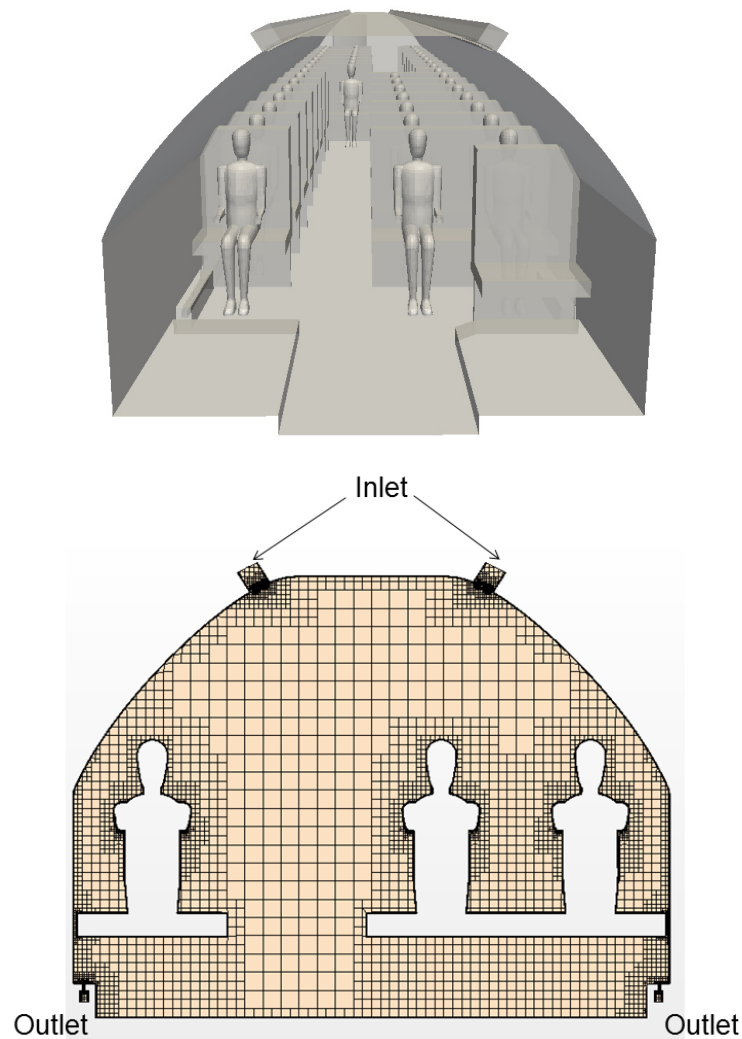


Figure 2: Cross section of the computational mesh and the model of the NGTII train cabin.

In Fig. 3 the geometrically complicated in- and outlets regions are presented. To resolve the aligned ribs in the inlet regions and the channels in the cabin outlets the meshes were refined as shown in Fig. 3 (left) for an inlet cross-section. In Fig. 3 (right) channels in a plane through the outlet channel are presented which were resolved in the mesh as well.

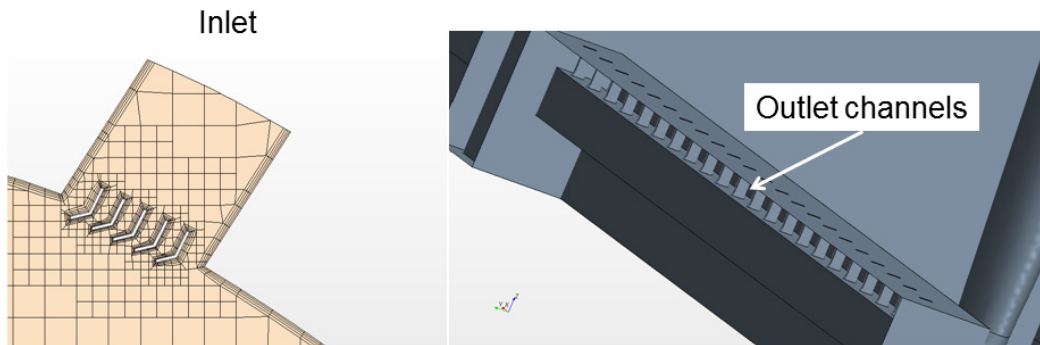


Figure 3: Details of in- and outlet geometry.

The conducted turbulent flow simulations include modelling of the thermal surface to surface radiation. They were carried out with the “buoyantBoussinesq” solver of OpenFOAM provided by Engys, which integrates the RANS equations together with the $k-\omega$ /SST model. The computed velocity and temperature fields in the train cabin are presented in Fig. 4, where streamlines of the mean velocity emerging from the inlet and the resulting surface temperature distributions are visualized.

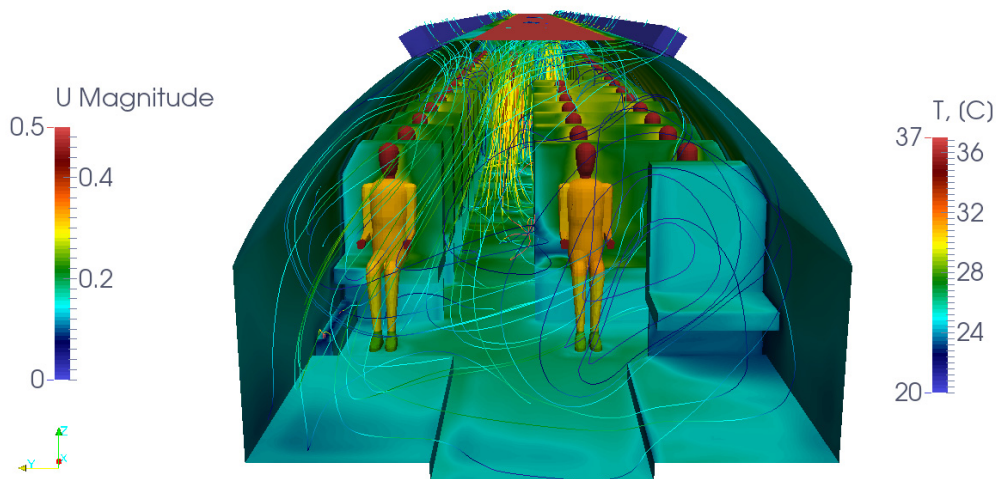


Figure 4: Predicted streamlines emerging from inlet surfaces and surface temperature distribution in the NGTII cabin

The numerical results reveal that an inhomogeneous temperature distribution develops in the cabin. In the Fig. 5 the surface temperature distribution on the passengers, seats and floor is shown. Additionally, the iso-surface of air temperature $T = 22\text{ C}^\circ$ is presented. Due to the asymmetric seating arrangement in the cabin, the flow is highly three-dimensional and unsteady.

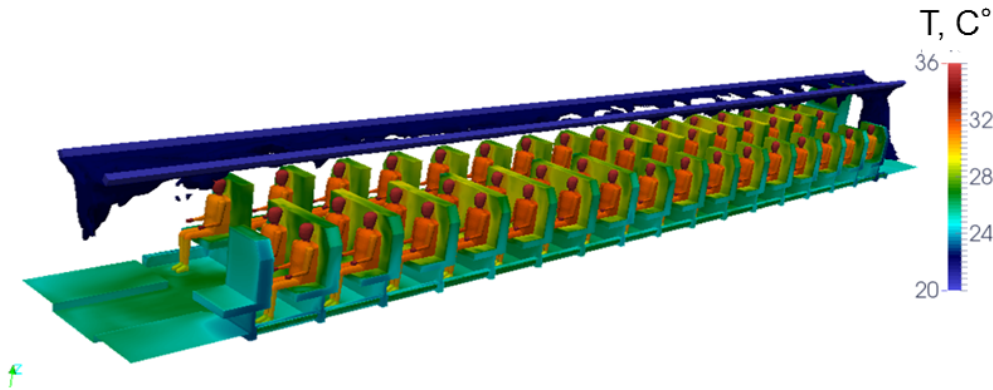


Figure 5: Surface temperature distribution on passengers, seats and floor with air surface temperature of $T = 22\text{ C}^\circ$.

As mentioned above, heat flux densities on the passenger's surfaces are first computed and then passed on to the finite-element code THESEUS-FE. The latter updates the surface body temperatures with the FIALA-Manikin model. The RANS simulations are continued with these new temperature boundary conditions at the passenger surfaces. Additionally, several comfort parameters such as the perceived temperature are determined with THESEUS-FE. Fig. 6 reflects the calculated temperature distribution in cross-section of train cabin in combination with the distribution of the Zhang local comfort indices, which display the well-being of passengers. The comfort feeling of passengers depends not only on the temperature distribution, but also on the air velocity. The distribution of the Zhang local comfort index reveals that in spite of the inhomogeneous internal cabin flow, the comfort values on the passenger body elements are lying between "comfortable" and "just comfortable".

Additionally, the results show that the temperature distribution in the cabin is inhomogeneous. In the centre of the cabin it is considerably warmer than on the edges.

Finally, the computed comfort is reflected with local equivalent temperatures. Although the ISO 14505-2 contains guidelines for the assessment of the thermal conditions in automobiles, they can be also used for other enclosures with asymmetric thermal conditions. The equivalent temperature is the temperature of a homogeneous room with a radiation background temperature equal to the air temperature and low relative air speed.

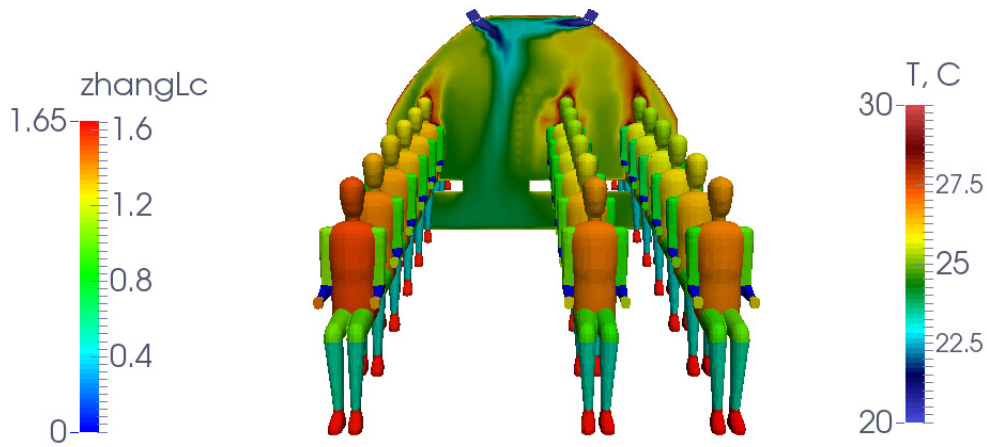


Figure 6: Temperature distribution in a cross-section and Zhang local indices on the passenger's surfaces.

In the Fig. 7 the local equivalent temperatures of three passengers in row 6 are presented. The passenger 61 and 63 are seated close to a window while passenger 62 is seated next to the aisle. The boundaries between comfort zones are indicated with lines. The body parts are indexed as follows: 15 – whole human body, 14 – head, 13 – torso, 12 – left upper arm, 11 – left lower arm, 10 – right upper arm, 9 – right lower arm, 8/7 – left/right hand, 6 – left upper leg, 5 – left lower leg, 4 – right upper leg, 3 – right lower leg and 2/1 – left/right foot.

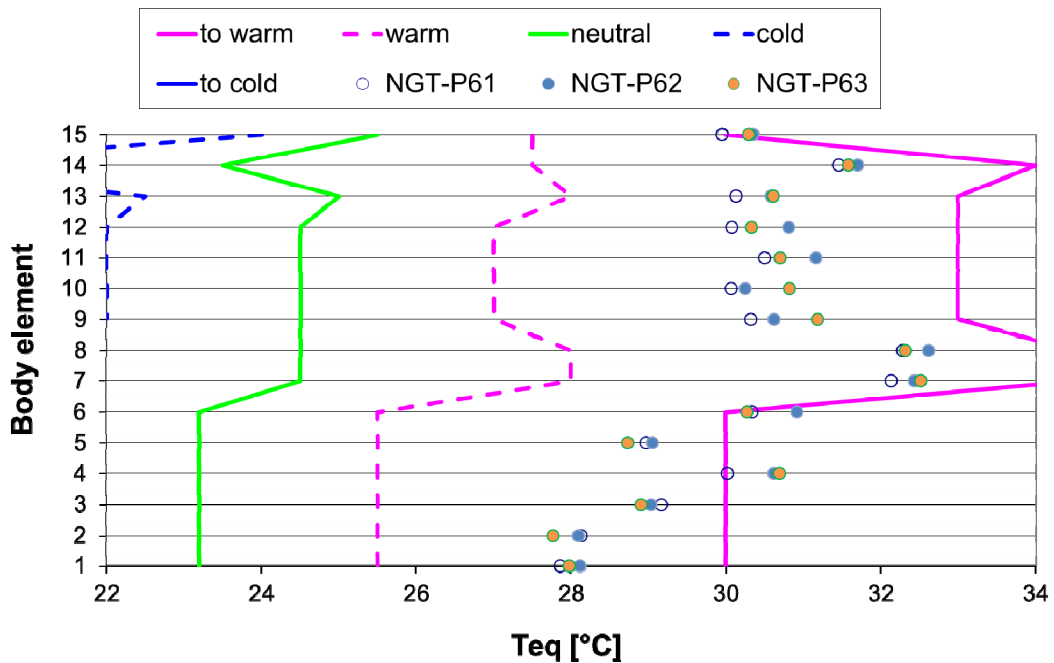


Figure 7: Equivalent temperature distribution on body element for passengers from row 6.

The ISO comfort zones, reflected in Fig. 7 as lines, were defined analysing a large number of experiments conducted for winter and summer conditions with samples of test persons and measurements of equivalent temperatures. Here we consider the summer comfort zones, and obtain that the predicted indices fall in the warm, but comfortable, zone for all passengers. The only exception are the upper legs which are in “too warm” zone. This means that a slightly lower inlet temperatures would probably improve the thermal comfort of the passengers for the considered case.

The equivalent temperature distribution in row 6 reveals that the air circulation of passenger 61 is better in agreement with the predicted Zhang local comfort indices presented in Fig. 8.

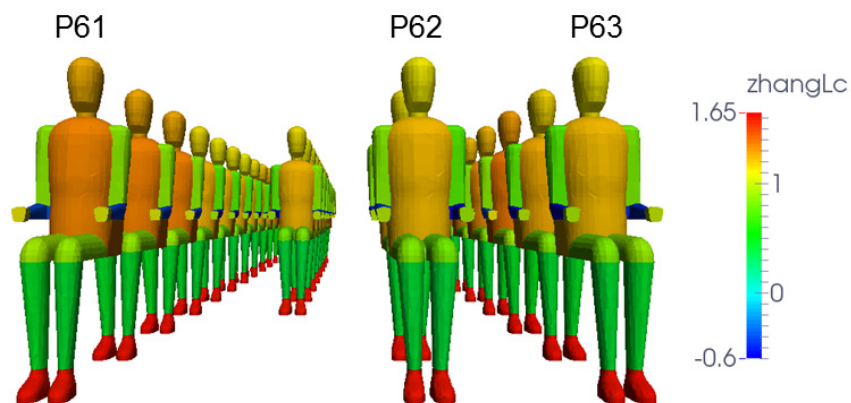


Figure 8: Zhang local comfort indices on the passengers. Row 6 is the first to see.

5 Conclusions

The presented numerical thermal comfort predictions are based on the solutions of the RANS equation. The latter are based on the Boussinesq approximation and on the modelling of the thermal surface to surface radiation in train cabin as well as the coupling with the finite element code THESEUS. The used simulation approach allows to simulate the heat transport within the passengers, the perceived temperatures and the passenger comfort. The analysis of the results further revealed that a proper modelling of the clothing is of particular importance for a realistic prediction of thermal radiation within the cabin. Finally, the conditions in the considered train cabin have been found to be comfortable.

References

- [1] M. Rütten, M. Konstantinov, C. Wagner, “ Analysis of Cabin Air Ventilation in the Do728 Test Facility based on High-Resolution Thermography”, Deutsches Luft- und Raumfahrtkongress 2008, Darmstadt, 2008.
- [2] M. Konstantinov, M. Rütten, M. Lambert, C. Wagner, „Strahlung als wesentlicher Faktor der numerischen Simulation von Flugzeugkabinen-

- innenströmungen für Komfortvorhersagen“, Deutsches Luft- und Raumfahrtkongress 2009, ID: 121285, Aachen, 2009.
- [3] D. Müller, M. Schmidt, S. Otto, I. Gores, M. Markwart, “Fully Automated Simulation Process for Comfort Predictions in Aircraft Cabins”, IndoorAir 2008, Copenhagen, 2008.
- [4] THESEUS-FE Theory Manual, Version 4.0. P+Z Engineering GmbH, Munich, 2011.
- [5] D. Fiala, “Dynamic Simulation of Human Heat Transfer and Thermal Comfort”, Ph. D. Thesis. Inst. Energy and Sustainable Development, De Montfort University Leicester, 1998.
- [6] D. Fiala, K.J. Lomas, M. Stohrer, “Computer prediction of human thermoregulatory responses to a wide range of environmental conditions”, Int. J. Biometeorol. 45, 143-159, 2001.
- [7] H. Zhang, E. Arens, C. Huizenga, T. Han, “Thermal Sensation and Comfort Models for Non-uniform and Transient Environments: Part I: Local Sensation of Individual Body Parts”, J. Building and Environment 45, 380-388, 2010.
- [8] H. Zhang, E. Arens, C. Huizenga, T. Han, “Thermal Sensation and Comfort Models for Non-uniform and Transient Environments: Part II: Local Comfort of Individual Body Parts”, J. Building and Environment 45, 389-398, 2010.
- [9] E.A. McCullough, B.W. Jones, J. Huck, “A Comprehensive Data Base for Estimating Clothing Insulation”. ASHRAE Trans. 91, 316-328, 1985.
- [10] M. Konstantinov, W. Lautenschlager, C. Wagner, “Numerical Simulation of Thermal Comfort in Aircraft Cabins”, 4th International Workshop on Aircraft System Technologies AST 2013, Hamburg, 231-240, 2013.